ACS APPLIED MATERIALS & INTERFACES

Research Article

www.acsami.org

# Improved Mechanical and Electronic Properties of Co-assembled Folic Acid Gel with Aniline and Polyaniline

Priyadarshi Chakraborty, Partha Bairi, Bappaditya Roy, and Arun K. Nandi*

Polymer Science Unit, Indian Association for the Cultivation of Science, Jadavpur, Kolkata 700032, India

Supporting Information

**ABSTRACT:** Co-assembled folic acid (**F**) gel with aniline (**ANI**) (**ANI**:**F** = 1:2, w/w) is produced at 2% (w/v) concentration in water/DMSO (1:1, v/v) mixture. The gel is rigid and on polymerization of the gel pieces in aqueous ammonium persulfate solution co-assembled folic acid - polyaniline (**F-PANI**) gel is formed. Both the co-assembled **F-ANI** and **F-PANI** gels have fibrillar network morphology, the fiber diameter and its degree of branching increase significantly from those of **F** gel. WAXS pattern indicates co-assembled structure with the **F** fiber at the core and **ANI**/**PANI** at its outer surface and the co-assembly is occurring in both **F-ANI** and **F-PANI** systems through noncovalent interaction of H-bonding and $\pi$ stacking processes between the components. FTIR and UV−vis spectra characterize the doped PANI formation and the MALDI mass spectrometry indicates the degree of polymerization of polyaniline in the range 24-653. The rheological experiments support the signature of gel formation in the co-assembled state and the storage ($G'$) and loss ($G''$) modulii increase in the order **F** gel< **F-ANI** gel < **F-PANI** gel, showing the highest increase in $G' \approx 1100\%$ for the **F-PANI** gel. The stress at break, elasticity, and stiffness also increase in the same order. The dc-conductivity of **F-ANI** and **F-PANI** xerogels is 2 and 7 orders higher than that of **F** xerogel. Besides, the current ($I$)−voltage ($V$) curves indicate that the **F**-xerogel is insulator, but **F-ANI** xerogel is semiconductor showing both electronic memory and rectification; on the other hand, the **F-PANI** xerogel exhibits a negative differential resistance (NDR) property with a NDR ratio of 3.0.

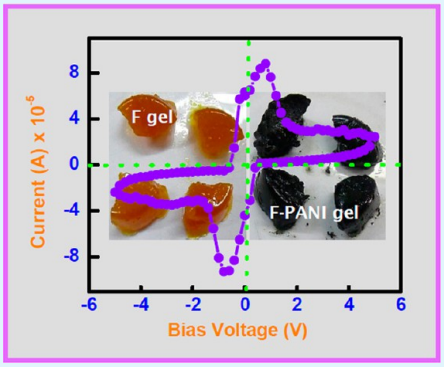


**KEYWORDS:** *supramolecular gel, folic acid, polyaniline, rheology, rectification, negative differential resistance*

## INTRODUCTION

In recent years, hybrid soft materials (gels) have received fascinating attention because of their interesting material properties.[1−5] This type of hybrid soft materials can be prepared by adding surfactants, polymers and nanoparticles to the gelator molecules which promote much improved physical and mechanical properties.[6−11] In this context, conductive gels have good prospect as an excellent functional material because of their applications in fuel cells, super capacitors, dye-sensitized solar cells, and rechargeable lithium batteries.[12−16] Fabrication of conducting gels can be achieved by adding conductive particles to the gel matrix,[17] producing the gels directly from conducting polymers[18−24] or incorporating conducting polymers into the network structure of the gels.[25,26] They can also be engineered via blending, double-network (DN) and triple network (TN) formation,[27−30] however, the blending method usually weakens the mechanical properties of the conducting composite gels.[31] There are some reports on preparation of conductive hydrogels by in situ polymerization[32,33] and Xia et al. have recently reported a polyaniline reinforced conducting hydrogel by polymerization of aniline in poly(acrylic acid) (PAA) hydrogel showing enhanced mechanical and electrical properties.[34] However the reports of in situ polymerization of aniline in supramolecular gels are a few in literature.[35,36]Also the mechanical and electrical properties of the supramolecular gel−polyaniline hybrid material are yet to be investigated. Combination of the soft nature, high tunability, and thermoreversibility of the supramolecular gels with the electrical properties of polyaniline can give birth to new kind of next-generation smart functional materials.

Folic acid (vitamin $B_9$) (**F**) is an important biomolecule containing two carboxylic acid functional groups (Scheme 1). It forms a supramolecular gel in 1:1 water/DMSO mixture (v/v).[37] Here, we have synthesized polyaniline in this supramolecular gel by absorbing aniline on fibers of folic acid producing co-assembled gel, followed by polymerization. The folic acid-polyaniline (**F-PANI**) and folic acid aniline (**F-ANI**) (Scheme 1) co-assembled gels not only show enhanced mechanical and conducting properties from the parent gel but also exhibits interesting electronic memory, rectification and negative differential resistance (NDR) properties. To the best of our knowledge, this is a unique and first time report of enhancement of mechanical and electrical properties of a supramolecular gel by in situ polymerization of aniline.

**Received:** December 19, 2013
**Accepted:** February 4, 2014
**Published:** February 4, 2014

   dx.doi.org/10.1021/am405868j | *ACS Appl. Mater. Interfaces* 2014, 6, 3615−3622

**Scheme 1. Chemical structures of Folic acid and Polyaniline**

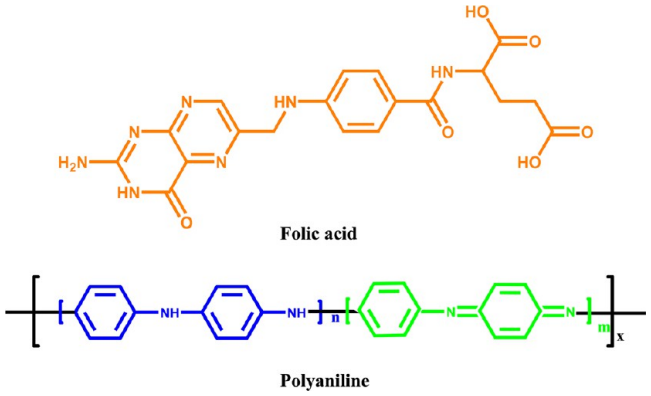


## EXPERIMENTAL SECTION

**Materials.** Folic Acid (**F**) was purchased from SRL, Mumbai, India, and was used as-received. Ammonium persulphate (APS) was purchased from MERCK, Mumbai, and was used as-received. The solvent dimethyl sulfoxide (DMSO, Rankem) was purchased from RFCL, New Delhi, India, and water was double-distilled before use. Aniline monomer (MERCK Chemicals) was distilled under reduced pressure prior to use.

**Preparation of F, F-ANI and F-PANI gels.** The **F** gel was prepared, throughout the work, by dissolving folic acid (80 mg, 2 % w/v) in a DMSO:water mixture at a volume ratio of 1:1, at 70 °C in a capped tube and it was then cooled to 30 °C producing a gel. The gel formation was recognized by the cessation of flow on inverting the tube. A stock of anilinium chloride solution was prepared by dissolving 0.4 mL of aniline in 20 mL of 0.2 N HCl. Folic acid (80 mg) was taken in a screw capped vial containing 2 mL of anilinium chloride solution (**ANI:F** =1:2, w/w) and 2 mL of DMSO, and was heated to dissolve completely. The vial was kept at room temperature and gel formation was observed within 2−3 min. Like the **F** gel, the aniline-absorbed **F** gel (**F-ANI**) (2% w/v) possesses high mechanical strength and it can be slashed into pieces (Figure 1). When the slashed pieces were

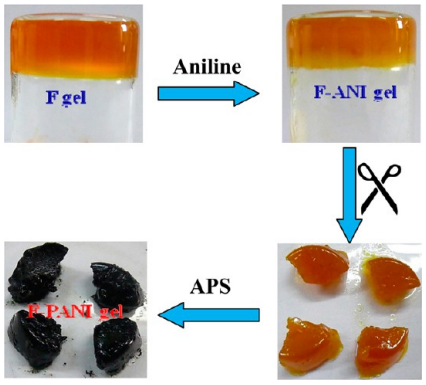


**Figure 1.** Physical appearances of the gels and the polymerization of **F-ANI** gel with APS producing **F-PANI** gel.

dipped into an aqueous solution of ammonium persulphate ($(NH_4)_2S_2O_8$, APS, 300 mg, 1.3 mmol) and aged at 30° C for 24 h, polymerization of aniline occurred. A prominent color change of the gel pieces from orange-yellow to deep green was observed. The folic acid-polyaniline (**F-PANI**) gel pieces (Figure .1) were washed repeatedly with water to remove APS and oligoaniline.[38] The xerogels were prepared by drying the gel in air at room temperature (30° C) for 2 weeks and they were finally dried at 30° C in vacuum for 3 days.

**Microscopy.** The morphology of all the gels was investigated by transmission electron microscopy (TEM). Small portions of the **F**, **F-ANI**, and **F-PANI** gels were diluted and were drop-casted on carbon-coated copper grid (300 mesh) and the samples were dried in open air at 30 °C. Finally, the samples were kept in a vacuum for 2 days at 30 °C before the experiment. SEM images of the samples were observed through an FESEM instrument (JEOL, JSM 6700F) operating at 5 kV after platinum coating. Small portions of the gels were placed on a glass coverslip and dried in air at 30 °C for a week and finally in a vacuum.

**Spectroscopy.** The UV−-vis spectra of the samples were recorded with a Hewlett-Packard UV−vis spectrophotometer (model 8453) in a cuvette of 0.1 cm path length. The concentration of the samples was 0.025 %. The FT-IR spectra of the xerogels were recorded using KBr pellets in a Perkin Elmer FT-IR instrument (FT-IR-8400S).

**Diffraction Study.** Wide angle X-ray scattering (WAXS) experiments of **F**, **F-ANI**, and **F-PANI** xerogels were performed in a Bruker AXS diffractomer (model D8 Advance) using a Lynx Eye detector. The instrument was operated at a 40 KV voltage and at a 40 mA current. Samples were placed on glass slides and were scanned in the range of $2\theta = 4-40°$ at the scan rate of 0.5 s/step with a step width of 0.02°.

**MALDI-TOF.** MALDI-TOF spectra of NMP solution of the **F-PANI** and **F** gel were made with a MALDI TOF Ultraflextreme (Bruker Daltonics) instrument using 2,5-dihydroxybenzoic acid (DHB) as matrix.

**Rheology.** To understand the mechanical property of the **F**, **F-ANI**, and **F-PANI** gels rheological experiments were performed with an advanced rheometer (AR 2000, TA Instrument, USA) using cone plate geometry on a peltier plate. The diameter of the plate was 40 mm and the cone angle was 4° with a plate gap of 121$\mu$m.

**Conductivity.** The dc-conductivity of the dried gel samples was measured by two-probe method at 30 °C with an electrometer (Keithley, model 617). For electrical conductivity measurements, the xerogels were pressed to make pellets in a press. Thickness ($d$) of the pellets is measured at four different positions using a screw gauge, and the results are averaged. The conductivity ($\sigma$) is measured from the relation

$$\sigma = (1/R)(d/a)$$

Where $R$ is the resistance of the sample obtained from the electrometer and $a$ is the area of the electrode.

## RESULTS AND DISCUSSION

**Characterization of F, F-ANI, and F-PANI Gels.** FTIR spectra are used to comprehend the nature of supramolecular interactions of folic acid gel with aniline and polyaniline and the FTIR spectra of **F**, **F-ANI**, and **F-PANI** xerogels are presented in Figure 2. Intermolecular H-bonding between the functional groups like −COOH, −OH, and $-NH_2$ groups having vibrational peaks in the region 3000−3600 $cm^{-1}$ in pure **F** powder combine to form a broad band at 3399 $cm^{-1}$ producing the **F** gel.[37] In the **F-ANI** xerogel this band is shifted to 3404 $cm^{-1}$ indicating supramolecular interactions between the folic acid and aniline. Also the vibrational peak of carbonyl stretching

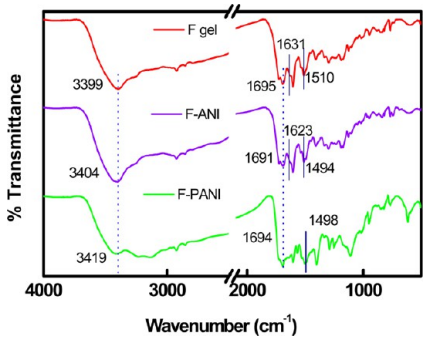


**Figure 2.** FTIR spectra of **F**, **F-ANI**, and **F-PANI** xerogels.


dx.doi.org/10.1021/am405868j | ACS Appl. Mater. Interfaces 2014, 6, 3615−3622

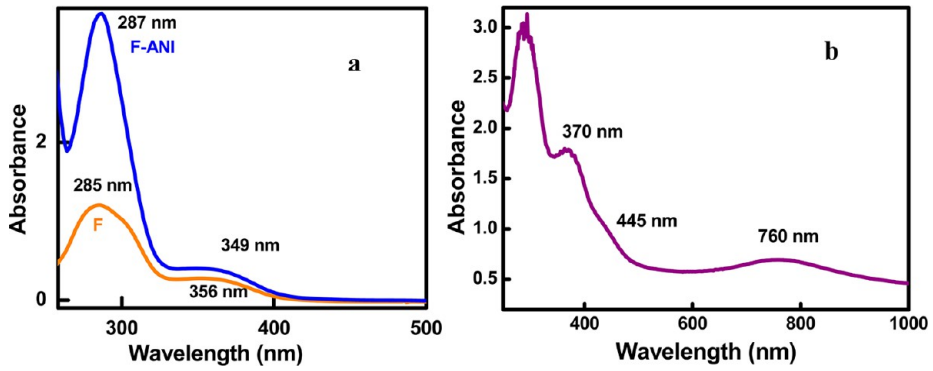


**Figure 3.** UV−vis spectra of (a) **F** and **F-ANI** and (b) **F-PANI** gel in DMSO/water (1:1 v/v) mixture.

of −COOH group of **F** xerogel at 1695 $cm^{-1}$ is shifted to 1691 $cm^{-1}$ in the **F-ANI** xerogel indicating H-bonding between the two components. During the xerogel formation, it is possible that the structure of **F-ANI** co-assembled state is completely retained. This is the probable cause of the observed shift of the above two bands of **F** in the xerogel state. In the **F-PANI** xerogel, the 3399 $cm^{-1}$ band of **F** xerogel is further shifted to 3419 $cm^{-1}$ signifying supramolecular interaction between **F** with **PANI.** Thus in all the gels this band is at lower positions than the −O−H stretching frequency (3543 $cm^{-1}$) of **F** powder.[39] The lower shift in **F-PANI** compared to that of **F-ANI** is probably due to the lower interaction because of conformational restriction of long **PANI** chain. Figure S1 in the Supporting Information represents the enlarged FTIR spectra of the **F-PANI** xerogel in the range 500−2000 $cm^{-1}$. Typical stretching bands at 767 and 1110 $cm^{-1}$ ($\gamma_{C-H}$ aromatic out of plane and the in plane deformation), 1291 $cm^{-1}$ ($\gamma_{C-N}$ for the secondary aromatic amine), 1501 $cm^{-1}$ ($\gamma_{C=C}$ for benzenoid rings), 1568 $cm^{-1}$ ($\gamma_{C=C}$ for quinoid rings) points to the formation of PANI inside the **F** gel.[40,41] A hump is observed at 1150 $cm^{-1}$ and the shift of 10 nm of N═Q═N vibration of PANI is due to the doping of quinonoid (*Q*) structure of PANI by folic acid.[41] The absorption band of phenyl ring in **F** gel is 1510 $cm^{-1}$[39] and in **F-ANI** gel it is 1494 $cm^{-1}$ and in **F-PANI** gel it is 1498 $cm^{-1}$. Thus in both cases there is a shift of the ring vibration to lower energy suggesting the delocalization of $\pi$-clouds of phenyl ring of **F** due to the $\pi-\pi$ interaction with the phenyl ring of **ANI** and **PANI.** It is important to note that in the case of **F-ANI**, the shift to lower energy is higher than that of **F-PANI** because of better $\pi$-stacking for the monomeric structure; on polymerization, some difficulty arises because of the formation of rigid covalent structure. (The presence of $\pi-\pi$ stacking is also evidenced from broad WAXS diffraction peak at $2\theta$ = 27.2° discussed later). Also the hump at 1631 $cm^{-1}$ in **F** xerogel corresponds to the >C═O vibration of −CONH group and it is lower by 9 $cm^{-1}$ than that of **F** powder[39] because of the H-bonding interaction of amido hydrogen with the amide >C═O group of another **F** molecule.[42] It shifts to 1623 $cm^{-1}$ in the **F-ANI** gel, suggesting its better H-bonding interaction is probably due to more regular structure formation during co-assembly with aniline. Thus the co-assembly is occurring in both **F-ANI** and **F-PANI** systems through noncovalent interaction of H-bonding and $\pi$-stacking processes between the components.

Absorbance spectra of **F** and **F-ANI** solution in DMSO water mixture are presented in Figure 3a. **F** exhibits two absorption peaks at 285 and 356 nm which may be ascribed to the $\pi-\pi^*$ and n-$\pi^*$ transition, respectively.[37] In the **F-ANI** gel the $\pi-\pi^*$ transition is very intense and it is red shifted to 287 nm, suggesting the formation of co-assembly between **F** and aniline. UV−vis spectra of **F-PANI** gel in DMSO water mixture (Figure 3b) exhibit an absorption band at 370 nm that may by ascribed to the n−$\pi^*$ transition of **F**, which is red shifted by 14 nm probably because of the co-assembly. The hump at 445 nm is attributed to the polaron band to $\pi^*$ band transition of **PANI**, indicating the **PANI** is produced in the doped state. The 760 nm peak corresponds to the $\pi$-band to localized polaron band transition of doped **PANI** and the absence of any free carrier tail beyond it suggests the absence of delocalized polaron in the **F-PANI** co-assembled gel.[41,43−46] So from the UV−vis results, it is apparent that polyaniline is doped and the hump at 1150 $cm^{-1}$ in FTIR spectrum (see Figure S1 in the Supporting Information) also supports the doping state of **PANI**. We have made a controlled experiment where the **F** gel is treated with **APS** (1.3 mmol) for 24 h without the presence of aniline. No significant changes in UV−vis spectra (see Figure S2 in the Supporting Information) are observed. The two absorption peaks at 285 and 356 nm, ascribed to the $\pi-\pi^*$ and n−$\pi^*$ transition, respectively, of the **F** gel, remain intact after APS treatment, indicating the absence of any oxidation of the folic acid host matrix under the experimental conditions used to produce **F-PANI** gel.

WAXS patterns of the xerogels (Figure 4) signify different crystalline structures of **F**, **F-ANI**, and **F-PANI** gels. The **F** spectrum is almost retained in **F-ANI** gel; in addition, some new sharp crystalline peaks have appeared signifying a small structural change in **F** gel after addition of aniline. The reason may be ascribed to the supramolecular organization of aniline molecules surrounding **F** fibers by interaction through its

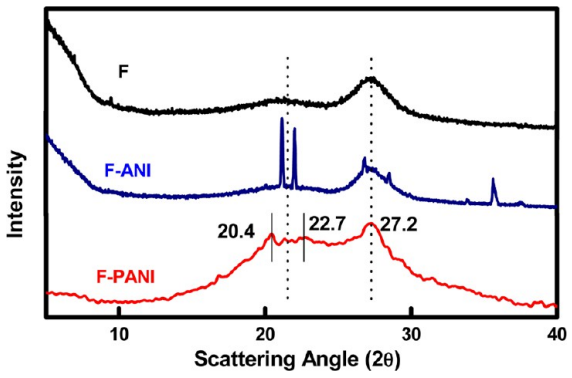


**Figure 4.** WAXS patterns of **F**, **F-ANI**, and **F-PANI** xerogels.


dx.doi.org/10.1021/am405868j | ACS Appl. Mater. Interfaces 2014, 6, 3615−3622

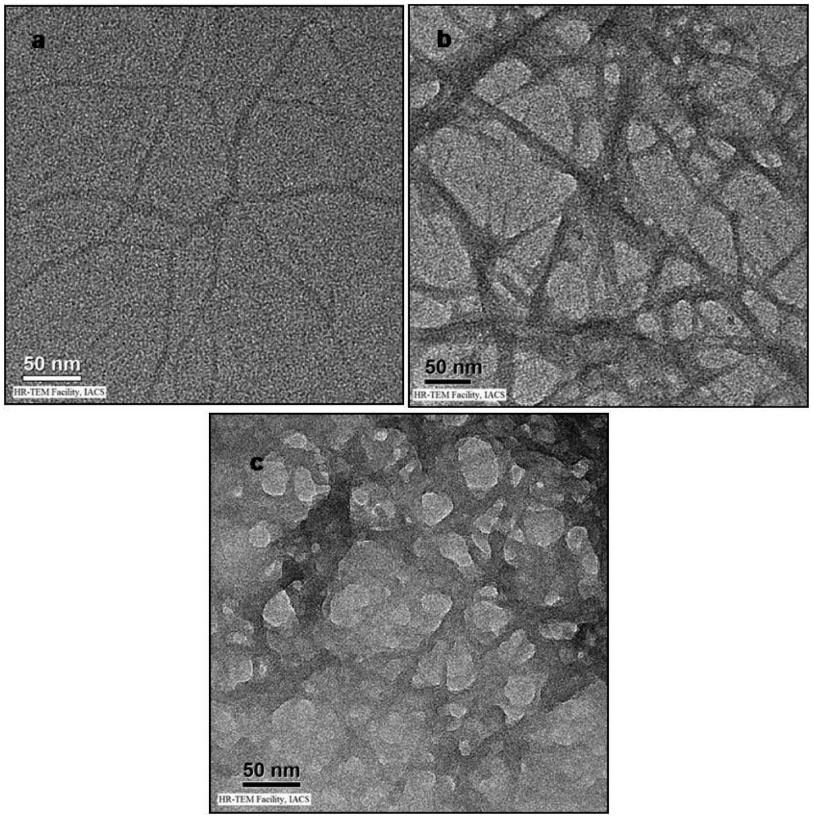


**Figure 5.** TEM images of (a) **F**, (b) **F-ANI** and (c) **F-PANI** gel.

−COOH groups, which prefer to remain at the periphery of the **F** fiber because of the polar nature of the solvent. This may result in the formation of co-assembled aniline crystals on **F** fiber resulting the sharp peaks of the **F-ANI** diffractogram. **F-PANI** gel exhibits a diffraction peak centred at $2\theta = 20.4^0$ ascribed to the periodicity parallel to the **PANI** chains.[38] The absence of sharp peaks observed in **F-ANI** in the **F-PANI** xerogel suggests the polymerization of adsorbed aniline may disfavor the ordered crystallite formation rather co-assembled disordered crystals of **PANI** chains adhering to the **F** fibers are produced. A careful analysis can recognize an additional broad peak ($2\theta \approx 22.7°$), and this broadness may be due to the partial amorphous nature of the **PANI** chains. The broad diffraction peak at $2\theta = 27.2°$ is present in all the three **F**, **F-ANI**, and **F-PANI** gels and it is for the interlayer spacing for $\pi-\pi$ stacking in the **F** gels.

**MALDI-TOF analysis.** Mass spectrometric methods, e.g., MALDI-TOF and ESI-TOF have been recently utilized for determining the molecular weight of soluble oligomers of polyaniline.[47−49] Here, we have used the MALDI-TOF method to determine the molecular weight of polyaniline synthesized inside the **F** gel matrix. Figure S3a, b in the Supporting Information presents the MALDI-TOF spectrum of a NMP solution of the **F-PANI** gel using 2,5-dihydroxybenzoic acid (DHB) as matrix. Figure S3a in the Supporting Information (range of $m/z$ values = 1500−20 000) shows a Gaussian type of pattern showing a maximum at $m/z$ = 5556. However, Figure S3b in the Supporting Information (range of $m/z$ values = 20 000−70 000) shows distinct peaks at $m/z$ = 21 179, 28 091, 34 038, 37 133, 44 990, and 59 428. Thus both these figures suggest the formation of both low and high molecular weight polyaniline inside the **F** gel as by dividing the $m/z$ value (taking $z = 1$) with the monomer molecular weight (91) the degree of polymerization from 24 to 653 are observed. The MALDI-TOF spectrum of a NMP dispersion of the **F** gel (similarly prepared to that of **F-PANI** gel) using DHB as matrix is carried out and no distinct peaks in the range of $m/z$ values = 2000−20000 and 20 000−70 000 are observed in the spectra (see Figure S3c,d in the Supporting Information). The results indicate that **F** does not self aggregate in NMP and the degree of polymerization values can therefore be attributed to the polyaniline produced in the **F**-gel.

**Morphology.** Transmission electron microscopy (TEM) was performed to investigate the morphological metamorphosis of **F** gel after addition of aniline and after its polymerization. In the TEM micrographs **F** gel shows fibrillar network morphology with an average fibrillar diameter 5.82 ± 2.15 nm (see Figure 5a and Figure S4a in the Supporting Information). The fibers are separated from each other with non frequent branching. However, after the addition of aniline, there is a change in the nature of fibers as evidenced from Figure 5b and Figure S4b in the Supporting Information) where the fibers become thicker with an average fibrillar diameter 10.12 ± 3.36 nm, also showing a greater degree of branching than the former. After polymerization of aniline, i.e., in the **F-PANI** gel, fibrillar network morphology is still observed (Figure 5c and Figure S4c in the Supporting Information) having average fibrillar diameter 12.44 ± 3.14 nm. The ∼2 times increase in the gel fiber diameter of **F-ANI** gel compared to that of **F** gel suggests an ordered arrangement of aniline molecules surrounding the **F** fibers through an interaction between the $-NH_2$ group of **ANI** and −COOH group of **F**, followed by self assembly formation. The diameter of **F-PANI** gel increases by ∼20% from that of **F-ANI** gel and

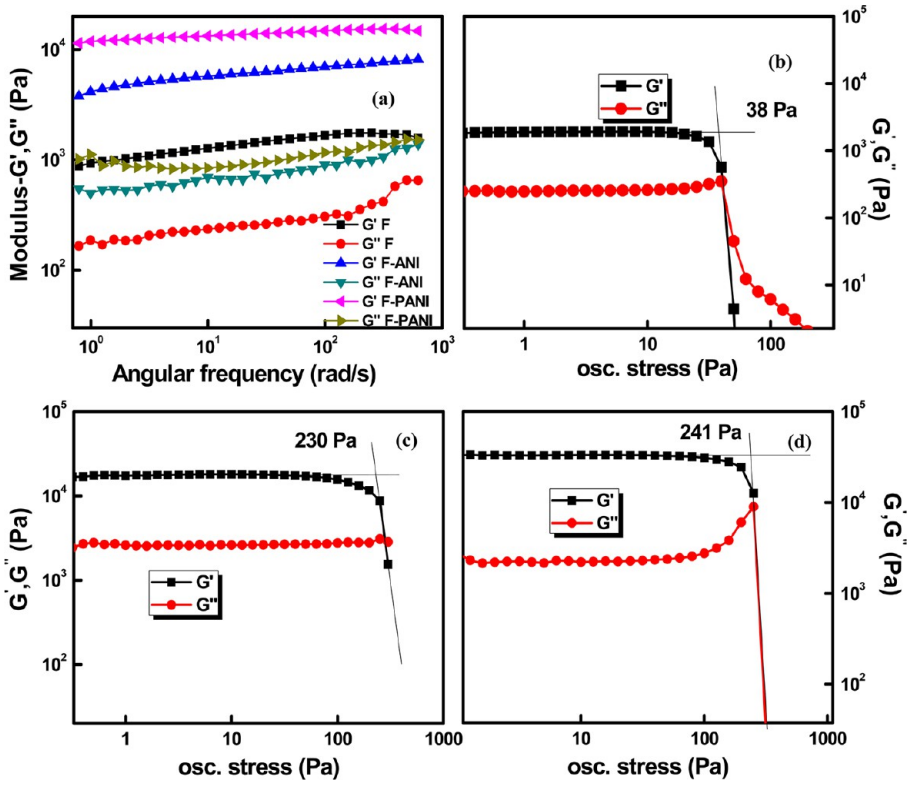


**Figure 6.** (a) Frequency-dependent oscillatory rheology of the gels and stress dependency of storage and loss modulus (b) **F** gel, (c) **F-ANI** gel, and (d) **F-PANI** gel at a frequency of 1 Hz.

probably polymerization of absorbed aniline imports some disorder including branching of PANI chains. The low-magnification TEM images (see Figure S4a–c in the Supporting Information) clearly indicates that the branching density increases in **F-ANI** and **F-PANI** gels from that of **F** gel. The FESEM micrographs are also presented in Figure S5 in the Supporting Information and here also an increase of branching density is clearly noticed in **F-ANI** and **F-PANI** co-assembled gels than that of **F** gel. The fibrillar branched network structure of **F-PANI** gel may arise from the formation of shell type polyaniline nanostructures surrounding the **F** gel fibers, which may remain as core (cf. WAXS results).

**Mechanical properties.** Gels are viscoelastic materials and they posses the intrinsic property of storing and dissipation of energy. The storage modulus ($G'$) indicates the amount of energy stored in the system and the loss modulus ($G''$) indicates the amount of energy dissipated within the system under the application of oscillatory stress. In the gel state $G' > G''$ and $G'(\omega) \approx \omega^0$, where $\omega$ is the angular frequency. The change in branching density affects the rheological properties (Figure 6, Table 1). The dynamic frequency sweep experiments (Figure 6a) of **F**, **F-ANI**, and **F-PANI** gels at a concentration of 2% (w/v) show a wide linear viscoelastic region (LVR). Also the value of storage modulus (G′) is considerably higher than that of the loss modulus ($G''$) in each case confirming their gel state. It is interesting to note that the $G'$ of the gels increases in the order **F** < **F-ANI** < **F-PANI**, indicating that the gel strength also follows the same order. The highest increase in $G'$ is 1100% for the **F-PANI** gel from that of **F** gel, which is due to the polyaniline-coated **F** nanofibers acting as a better reinforcing agent because of stronger co-operative supramolecular interactions with **F** than that of the monomer aniline. The covalent bond of **PANI** chain facilitates easier dissipation of energy than through the noncovalent bond ($\pi$–$\pi$ interactions) of adsorbed aniline molecules in **F-ANI** system. Stress sweep experiments (Figure 6b–d) reveal that the **F** gel breaks at an oscillator stress of 38 Pa but the **F-ANI** gel at 230 Pa and the **F-PANI** gel breaks at 241 Pa indicating very stiff nature of the **F-ANI** and **F-PANI** co-assembled gels because of a stronger cohesive force between F and the co-assembled **ANI** and **PANI** molecules.

**Table 1. Comparison of Rheological Data of F, F-ANI, and F-PANI Gels**

| samples | storage modulus G′ (Pa) | loss modulus G″(Pa) | elasticity $G' - G''$ (Pa) | stiffness $G'/G''$ | stress at break $\sigma^*$(Pa) |
|---|---|---|---|---|---|
| **F** gel | 1024 | 187 | 837 | 5.5 | 38 |
| **F-ANI** gel | 5160 | 581 | 4525 | 8 | 230 |
| **F-PANI** gel | 12640 | 882 | 11697 | 14 | 241 |

The elasticity ($G' - G''$) and stiffness ($G'/G''$)[42] of the gels, calculated from the rheological data, are presented in Table 1. Both the elasticity and stiffness increases in the order **F** gel < **F-ANI** gel < **F-PANI** gel. Because of the polymeric nature of **PANI**, the co-assembled **F-PANI** gel exhibits higher stiffness than **F-ANI** where co-assembly with aniline has increased the stiffness than that of **F** gel. The increase of elasticity in the above order may possibly be attributed to the increase of branch density of the fibers that follows the order **F** gel < **F-ANI** gel < **F-PANI** gel (Figure 5a–c). This type of improvement in the mechanical properties of the **F-ANI** gel over the **F** gel may be ascribed to the formation of a co-


dx.doi.org/10.1021/am405868j | ACS Appl. Mater. Interfaces 2014, 6, 3615–3622

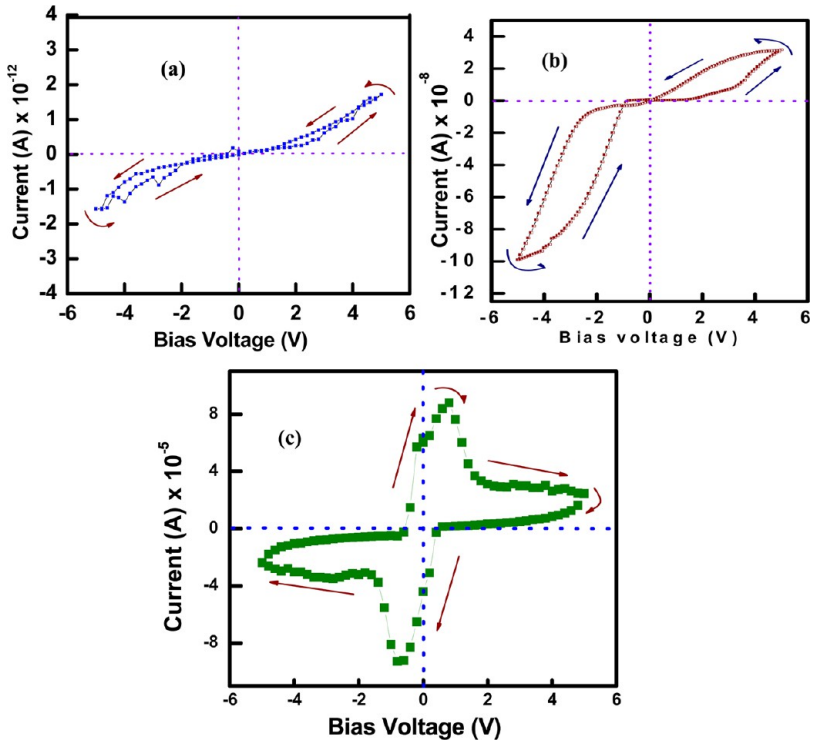


**Figure 7.** *I*–*V* characteristic curves of (a) **F**, (b) **F-ANI**, and (c) **F-PANI** xerogel measured at 30 °C.

assembled branched fibrillar structure resulting in stronger cohesive force between the fibrils of the network.

**Electrical Properties.** The dc conductivity values at 30 °C of **F**, **F-ANI**, and **F-PANI** xerogels, measured by two probe method, are $5 \times 10^{-12}$, $2 \times 10^{-10}$, and $1.4 \times 10^{-5}$ S/cm. The reason in the two orders increase in conductivity of **F-ANI** than that of **F** xerogel may be attributed to the $\pi$-stacking of co-assembled aniline molecules on the **F** fibers providing another path of conduction of the charge carriers. In the **F-PANI** xerogel, there are five orders of increase in conductivity from that of **F-ANI** gel, which may be attributed to the polymerization of aniline producing conjugated chain facilitating the easy movement of the charge carrier. The current–voltage (*I*–*V*) plot the **F**-xerogel exhibit almost an invariant current with increase of voltage (Figure 7a), like a typical insulator, but the **F-ANI** co-assembled xerogel exhibit the characteristics of electronic memory along with rectification property (Figure 7b). The probable reason of showing electronic memory may be attributed to the doped of aniline by folic acid, which acts as a matrix to store the doped charge and the supramolecular organized structure of co-assembled **F-ANI** system facilitates the process. This causes a bistable state and at a reverse bias higher current is observed than the forward bias till the charges are detrapped at a lower voltage of the reverse bias.[50] The same explanation can also be applied for the memory effect observed in the negative bias of the **F-ANI** system (Figure 7b). The rectification property (rectification ratio = 3.3) may arise because of p/n junction formation between doped **ANI** (p-type) by folic acid and the **F** assembly acts as n-type semiconductor because of the presence of the nonbonding electrons. Because of the co-assembly process between the **F** and doped **ANI** they intimately mix with each other producing effective p/n junctions at the bulk. On the other hand, it is interesting to note that **F-PANI** xerogel exhibits the characteristics of negative differential resistance (NDR) (Figure 7c), i.e., a decrease in current with increase in voltage starting at +0.8 and at −0.8 V for both the forward and backward bias. The NDR ratio (peak current/valley current) has the typical value of 3.0 in both positive and negative bias. We have repeated the experiment of **F-PANI** xerogel for different number of cycles and similar NDR property is observed in all the cases (see Figure S6 in the Supporting Information).

The **F-PANI** system can act as a very good semiconductor (due to conjugated chain of PANI) as well as it can act as a charge storage material because of $\pi$-stacking. Because of the stored space charge above 0.8 V, a decrease in current with the increase of voltage occurs until much higher voltage (2 V) is applied to release the space charge and it is usually called as negative differential resistance.[51] The negative hysteresis in the reverse bias is also due to the decrease in charge flow for the hindrance created by the absorbed space charges.

## CONCLUSION

In conclusion, we report here the co-assembled gel formation of **F** with **ANI** in water/DMSO (1:1, v/v) mixture. Both the **F** and **F-ANI** gels are rigid and on polymerization of gel pieces by dipping into aqueous APS solution; co-assembled **F-PANI** gel is formed. Both the co-assembled gels have fibrillar network morphology, the fiber diameter, and it's degree of branching increase significantly than those of **F** gel. The co-assembly is occurring in both F-ANI and F-PANI systems through non-covalent interaction of H-bonding and $\pi$ stacking processes between the components and the **F** fiber constitutes the core and **ANI**/**PANI** remains at its outer surface (shell). UV–vis and FTIR spectra characterize the doped polyaniline formation having degree of polymerization in the range of 24–653 and polymerization occurs though the adsorbed aniline molecules over the F fibers. The rheological experiments confirms the gel formation of **F**, **F-ANI** and **F-PANI** systems and both the storage ($G'$) and loss ($G''$) modulii increase in the order **F** gel <


dx.doi.org/10.1021/am405868j | ACS Appl. Mater. Interfaces 2014, 6, 3615–3622

**F-ANI** gel < **F-PANI** gel, showing the highest increase of $G' \approx$ 1100% for the F-PANI gel from that of **F** gel. The stress at break, elasticity, and stiffness also increase in the same order. The dc conductivity of **F-ANI** and **F-PANI** xerogels are 2 and 7 orders higher than that of **F** xerogel, respectively. The $I-V$ curves characterize that the **F**-xerogel as insulator, **F-ANI** xerogel as semiconductor possessing electronic memory and rectification, but, the **F-PANI** xerogel exhibits the NDR property with a NDR ratio of 3.0.

## ■ ASSOCIATED CONTENT

### Ⓢ Supporting Information

FTIR, UV-Vis, MALDI Mass, TEM (low resolution) , FESEM images and I−V curve of **F-PANI** co-assembled gel for repeated runs. This information is available free of charge via the Internet at http://pubs.acs.org/.

## ■ AUTHOR INFORMATION

### Corresponding Author

*E-mail: psuakn@iacs.res.in.

### Notes

The authors declare no competing financial interest.

## ■ ACKNOWLEDGMENTS

P.C, P.B acknowledges CSIR, New Delhi for providing the fellowship.

## ■ REFERENCES

(1) Shigekura, Y.; Chen, Y. M.; Furukawa, H.; Kaneko, T.; Kaneko, D.; Osada, Y.; Gong, J. P. Anisotropic Polyion-Complex Gels via Template Polymerization. *Adv. Mater.* **2005**, *17*, 2695−2699.

(2) Lee, H.; Mensire, R.; Cohen, R. E.; Rubner, M.F. Strategies for Hydrogen Bonding Based Layer-by-Layer Assembly of Poly(vinyl alcohol) with Weak Polyacids. *Macromolecules* **2012**, *45*, 347−355.

(3) Adhia, Y. J.; Schloemer, T. H; Perez, M. T.; McNeil, A. J. Using polymeric additives to enhance molecular gelation: impact of poly (acrylic acid) on pyridine-based gelators. *Soft Matter* **2012**, *8*, 430−434.

(4) Babu, S. S.; Praveen,V. K.; Ajayaghosh, A. Functional π-Gelators and Their Applications. *Chem. Rev.* dx.doi.org/10.1021/cr400195e

(5) Kartha, K. K.; Mukhopadhyay, R. D.; Ajayaghosh, A. Supramolecular Gels and Functional Materials Research in India. *CHIMIA International Journal for Chemistry* **2013**, *67*, 51−63.

(6) Kumar, V. R. R.; Sajini, V.; Sreeprasad, T. S.; Praveen, V. K.; Ajayaghosh, A.; Pradeep, T. Probing the Initial Stages of Molecular Organization of Oligo(*p*-phenylenevinylene) Assemblies with Monolayer Protected Gold Nanoparticles. *Chem. Asian J.* **2009**, *4*, 840−848.

(7) Srinivasan, S.; Babu, S. S.; Praveen, V. K.; Ajayaghosh, A. Carbon Nanotube Triggered Self-Assembly of Oligo(*p*-phenylenevinylene)s to Stable Hybrid π -Gels. *Angew. Chem. Int. Ed.* **2008**, *47*, 5746−5749.

(8) Dasgupta, D.; Srinivasan, S.; Rochas, C.; Ajayaghosh, A.; Guenet, J. M. Hybrid Thermoreversible Gels from Covalent Polymers and Organogels. *Langmuir* **2009**, *25*, 8593−8598.

(9) Herrikhuyzen, J. V.; George, S. J.; Vos, M. R. J.; Sommerdijk, N. A. J. M.; Ajayaghosh, A.; Meskers, S. C. J.; Schenning, A. P. H. J. Self-Assembled Hybrid Oligo(*p*-phenylenevinylene)−Gold Nanoparticle Tapes. *Angew. Chem. Int. Ed.* **2007**, *46*, 1825−1828.

(10) Rao, K. V.; Datta, K. K. R.; Eswaramoorthy, M.; George, S. J. Light-Harvesting Hybrid Hydrogels: Energy-Transfer-Induced Amplified Fluorescence in Noncovalently Assembled Chromophore−Organoclay Composites. *Angew. Chem. Int. Ed.* **2011**, *50*, 1179−1184.

(11) Rao, K. V.; Datta, K. K. R.; Eswaramoorthy, M.; George, S. J. Light-Harvesting Hybrid Assemblies. *Chem.—Eur. J.* **2012**, *18*, 2184−2194.

(12) Iwakura, C.; Murakami, H.; Nohara, N.; Furukawa, N.; Inoue, H. Charge−discharge characteristics of nickel/zinc battery with polymer hydrogel electrolyte. *J. Power Sources* **2005**, *152*, 291−294.

(13) Kato, T.; Okazaki, A.; Hayase, S. Latent gel electrolyte precursors for quasi-solid dye sensitized solar cells The comparison of nano-particle cross-linkers with polymer cross-linkers. *J. Photochem. Photobiol., A: Chemistry* **2006**, *179*, 42−48.

(14) Lin, J. M.; Wu, J. H.; Yang, Z.; Pu, M. Synthesis and Properties of Poly (acrylic acid)/Mica Superabsorbent Nanocomposite. *Macromol. Rapid Commun.* **2001**, *22*, 422−424.

(15) Nazmutdinova, G.; Sensfuss, S.; Schrödner, M.; Hinsch, A.; Sastrawan, R.; Gerhard, D.; Himmler, S.; Wasserscheid, P. Quasi-solid state polymer electrolytes for dye-sensitized solar cells: Effect of the electrolyte components variation on the triiodide ion diffusion properties and charge-transfer resistance at platinum electrode. *Solid State Ionics* **2006**, *177*, 3141−3146.

(16) Suzuki, M.; Hirasa, O. An approach to artificial muscle using polymer gels formed by micro-phase separation. *Adv. Polym. Sci.* **1993**, *110*, 241−261.

(17) Fan, S.; Tang, Q.; Wu, J.; Hu, D.; Sun, H.; Lin, J. Two-step synthesis of polyacrylamide/poly(vinyl alcohol)/polyacrylamide/graphite interpenetrating network hydrogel and its swelling, conducting and mechanical- properties. *J. Mater. Sci.* **2008**, *43*, 5898−5904.

(18) Morita, S.; Kawai, T.; Yoshino, K. The characteristics of a conducting polymer gel by use of a radical initiator. *J. Appl. Phys.* **1991**, *69*, 4445−4447.

(19) Donat, B. P.; Lairez, D.; Geyer, A.; de Viallat, A. Light and small angle neutron scattering studies of well-defined conducting gels. *Synth. Met.* **1999**, *101*, 471−472.

(20) Donat, B. P.; Quynh, A.V.; Viallat, A. Mechanisms of Deformation in Fully Conjugated Conducting Gels. Stretching and Swelling. *Macromolecules* **2000**, *33*, 5912−5917.

(21) Donat, B. P.; Viallat, A.; Blachot, J. F.; Fedorko, P.; Lombard, C. Swelling, elasticity and transport properties of conjugated covalent electronic conducting gels: role of network structure. *Synth. Met.* **2003**, *137*, 897−898.

(22) Jana, T.; Nandi, A. K. Sulfonic Acid-Doped Thermoreversible Polyaniline Gels: Morphological, Structural, and Thermodynamical Investigations. *Langmuir* **2000**, *16*, 3141−3147.

(23) Jana, T.; Nandi, A. K. Sulfonic Acid Doped Thermoreversible Polyaniline Gels. 2. Influence of Sulfonic Acid Content on Morphological, Thermodynamical, and Conductivity Properties. *Langmuir* **2001**, *17*, 5768−5774.

(24) Jana, T.; Chatterjee, J.; Nandi, A. K. Sulfonic Acid Doped Thermoreversible Polyaniline Gels. 3. Structural Investigations. *Langmuir* **2002**, *18*, 5720−5727.

(25) Fizazi, A.; Moulton, J.; Pakbaz, K.; Rughooputh, S. D. D. V.; Smith, P.; Heeger, A. Percolation on a Self-Assembled Network: Decoration of Polyethylene Gels with Conducting Polymers. *J. Phys. Rev. Lett.* **1990**, *64*, 2180−2183.

(26) González, I.; Vecino, M.; Muñoz, M. E.; Santamaría, A.; Pomposo, J. A. Electrically Conducting Gels Formed From Polyaniline/Ethylcellulose/m-Cresol Ternary Solutions. *Macromol. Chem. Phys.* **2004**, *205*, 1379−1384.

(27) Karbarz, M.; Gniadek, M.; Donten, M.; Stojek, Z. Intra-channel modification of environmentally sensitive poly(N-isopropylacrylamide) hydrogel with polyaniline using interphase synthesis. *Electrochem. Commun.* **2011**, *13*, 714−718.

(28) Zhang, X. T.; Chechik, V.; Smith, D. K.; Walton, P. H.; Duhme-Klair, A. K.; Luo, Y. J. Nanocomposite hydrogels—Controlled synthesis of chiral polyaniline nanofibers and their inclusion in agarose. *Synth. Met.* **2009**, *159*, 2135−2140.

(29) Dai, T. Y.; Qing, X. T.; Zhou, H.; Shen, C.; Wang, J.; Lu, Y. Mechanically strong conducting hydrogels with special double-network structure. *Synth. Met.* **2010**, *160*, 791−796.

(30) Dai, T. Y.; Qing, X. T.; Lu, Y.; Xia, Y. Y. Conducting hydrogels with enhanced mechanical strength. *Polymer* **2009**, *50*, 5236−5241.

(31) Siddhanta, S. K.; Gangopadhyay, R. Conducting polymer gel: formation of a novel semi-IPN from polyaniline and crosslinked poly(2-acrylamido-2-methyl propanesulphonicacid). *Polymer* **2005**, *46*, 2993−3000.
(32) Zhang, Y. W.; Zhao, J. X.; Li, X. F.; Tao, Y.; Wu, C. X. Swelling Behaviors of Polyaniline-Poly(Acrylic Acid) Hydrogels. *J. Donghua Univ.* **2005**, *22*, 100−104.
(33) Tang, Q. W.; Lin, J. M.; Wu, J. H.; Zhang, C. J.; Hao, S. C. Two-steps synthesis of a poly(acrylate−aniline) conducting hydrogel with an interpenetrated networks structure. *Carbohydr. Polym.* **2007**, *67*, 332−336.
(34) Xia, Y.; Zhu, H. Polyaniline nanofiber-reinforced conducting hydrogel with unique pH-sensitivity. *Soft Matter* **2011**, *7*, 9388−9393.
(35) Anilkumar, P.; Jayakannan, M. A Novel Supramolecular Organogel Nanotubular Template Approach for Conducting Nanomaterials. *J. Phys. Chem. B* **2010**, *114*, 728−736.
(36) Li, C.; Hatano, T.; Takeuchi, M.; Shinkai, S. Polyaniline superstructures created by a templating effect of organogels. *Chem.Comm.* **2004**, 2350−2351.
(37) Chakraborty, P.; Roy, B.; Bairi, P.; Nandi, A. K. Improved mechanical and photophysical properties of chitosan incorporated folic acid gel possessing the characteristics of dye and metal ion absorption. *J. Mater. Chem.* **2012**, *22*, 20291−20298.
(38) Rana, U.; Chakrabarti, K.; Malik, S. In situ preparation of fluorescent polyaniline nanotubes doped with perylene tetracarboxylic acids. *J. Mater. Chem.* **2011**, *21*, 11098−11100.
(39) Zhang, J.; Rana, S.; Srivastava, R.S.; Misra, R.D.K. On the chemical synthesis and drug delivery response of folate receptor-activated, polyethylene glycol-functionalized magnetite nanoparticles. *Acta Biomater.* **2008**, *4*, 40−48.
(40) Abdiryim, T.; Xiao-Gang, Z.; Jamal, R. Comparative studies of solid-state synthesized polyaniline doped with inorganic acids. *Mater. Chem. Phys.* **2005**, *90*, 367−372.
(41) Garai, A.; Kuila, B. K.; Nandi, A. K. Montmorillonite Clay Nanocomposites of Sulfonic Acid Doped Thermoreversible Polyaniline Gel: Physical and Mechanical Properties. *Macromolecules* **2006**, *39*, 5410−5418.
(42) Bairi, P.; Roy, B.; Routh, P.; Sen, K.; Nandi, A. K. Self-sustaining, fluorescent and semi-conducting co-assembled organogel of Fmoc protected phenylalanine with aromatic amines. *Soft Matter* **2012**, *8*, 7436−7445.
(43) Stejskal, J.; Kratochvil, P.; Radhakrishnan, N. Polyaniline dispersions 2. UV-Vis absorption spectra. *Synth. Met.* **1993**, *61*, 225−231.
(44) Huang, W. S.; MacDiarmid, A. G. Optical properties of polyaniline. *Polymer* **1993**, *34*, 1833−1845.
(45) Xia, Y.; Wiesinger, J. M.; MacDiarmid, A. G.; Epstein, A. Camphorsulfonic Acid Fully Doped Polyaniline Emeraldine Salt: Conformations in Different Solvents Studied by an UltravioletNisiblel Near-Infrared Spectroscopic Method. *J. Chem. Mater.* **1995**, *7*, 443−445.
(46) Ruokolainen, J.; Eerikainen, H.; Torkkeli, M.; Serimaa, R.; Jussila, M.; Ikkala, O. Comb-Shaped Supramolecules of Emeraldine Base Form of Polyaniline Due to Coordination with Zinc Dodecyl Benzenesulfonate and Their Plasticized Self-Organized Structures. *Macromolecules* **2000**, *33*, 9272−9276.
(47) Dolan, A.R.; Wood, T. D. Synthesis and characterization of low molecular weight oligomers of soluble polyaniline by electrospray ionization mass spectrometry. *Synth Met.* **2004**, *143*, 243−250.
(48) Dolan, A. R.; Wood, T. D. Analysis of Polyaniline Oligomers by Laser Desorption Ionization and Solventless MALDI. *J. Am. Soc. Mass Spectrosc.* **2004**, *15*, 893−899.
(49) Laska, J.; Widlarz, J. Spectroscopic and structural characterization of low molecular weight fractions of polyaniline. *Polymer* **2005**, *46*, 1485−1495.
(50) Hong, J.Y.; Jeon, S. O.; Jang, J.; Song, K.; Kim, S. H. A facile route for the preparation of organic bistable memory devices based on size-controlled conducting polypyrrole nanoparticles. *Org. Electron.* **2013**, *14*, 979−983.
(51) Routh, P.; Garai, A.; Nandi, A. K. Optical and electronic properties of polyaniline sulfonic acid−ribonucleic acid−gold nanobiocomposites. *Phys. Chem. Chem. Phys* **2011**, *13*, 13670−13682.